Quaternary International 418 (2016) 132–146

Contents lists available at ScienceDirect

Quaternary International

journal homepage: www.elsevier.com/locate/quaint

First results from the Late Pleistocene paleosols in northern Western Siberia: Implications for pedogenesis and landscape evolution at the end of MIS3

Vladimir Sheinkman [a, b, c], Sergey Sedov [a, c, d, *], Lyudmila Shumilovskikh [e, f], Elena Korkina [g, h], Sergey Korkin [g], Evgeniy Zinovyev [i], Alexandra Golyeva [j]

[a] Tyumen State Gas and Oil University, Russia
[b] Earth's Cryosphere Institute, SB RAS, Tyumen, Russia
[c] Tyumen State University, Tyumen, Russia
[d] Instituto de Geología, Universidad Nacional Autónoma de México, Mexico
[e] Department of Palynology and Climate Dynamics, Georg-August-University, Göttingen, Germany
[f] Laboratory of taxonomy and phylogeny of plants, Tomsk State University, Tomsk, Russia
[g] Nihznevartosk State University, Russia
[h] Saint Petersburg State University, Russia
[i] Institute of Plant and Animals Ecology, RAS, Urals Branch, Ekaterinburg, Russia
[j] Insitute of Geography, RAS, Russia

ARTICLE INFO

Article history:
Available online 23 April 2016

Keywords:
Last Glacial
Permafrost
Pollen and non-pollen palynomorphs
Botanical macroremains
Phytoliths
Fossil insects

ABSTRACT

Recent revision of the extent of Late Pleistocene glaciations in Northern Eurasia the justified search for the new paleopedological records in the center-north West Siberian Plain. We encountered paleosols in several exposures of the high alluvial terrace of the river Vakh (Middle Ob' basin), buried in the sequence of alluvial and lacustrine sediments. A paleosol dated to the end of Marine Isotope Stage (MIS) 3, Karga thermochron, was studied in detail in the key section "Zeleniy Ostrov". The paleosol demonstrates strong morphological evidence of gleysation and accumulation of plant residues, both processes indicating water logging and a reduced environment. The modern soil on top of the exposure is a typical Podzol, formed in under conditions of perfect soil drainage and no water excess, in agreement with current geological and geomorphological conditions. We suppose that permafrost was the main factor hampering percolation and switching redoximorphic processes in the paleosol, which thus was classified as a Reductaquic Cryosol. Presence of permafrost implies colder climate than the present one. Furthermore, neutral reaction, presence of neoformed calcium carbonate and abundance of silt fraction, which points to eolian sedimentation, suggest drier conditions. However, the studied paleosols differ considerably from the synchronous Chernozems found in the loess sequences of Southern Siberia. Paleobiological proxies such as pollen, plant macroremains, phytoliths and fossil insects indicate a tundra or tundra-steppe ecosystem (possibly with some forest stands), in good agreement with the paleopedological and sedimentary records.

1. Introduction

The environmental history of the glacial–interglacial cycle was significantly enriched during the last decades through involving new proxies with high temporal resolution such as Greenland ice cores (Andersen et al., 2004) further chronologically correlated with other detailed records (Svensson et al., 2006). The knowledge about the response of the continental ecosystems to these multi-scale global climatic changes is still patchy and insufficient. Thus, the search for the new detailed terrestrial paleoecological archives with high temporal resolution for the last glacial epoch is boosted.

Paleosols incorporated in the terrestrial sediments have proven to provide valuable paleoenvironmental information. In particular,

* Corresponding author. Instituto de Geología, Universidad Nacional Autónoma de México, Ciudad Universitaria, del. Coyoacán, Cd. México, CP 04510, Mexico.
E-mail addresses: serg_sedov@yahoo.com, sergey@geologia.unam.mx (S. Sedov).

http://dx.doi.org/10.1016/j.quaint.2015.12.095
1040-6182/

loess-paleosol sequences of Eurasia were interpreted as a record of glacial–interglacial cycles throughout the Quaternary; well developed loessic paleosols were attributed to interglacials and correlated with the odd-numbered MIS (e.g. Kukla and An, 1989; Bronger et al., 1998; Dodonov et al., 2006). Much weaker interstadial paleosols were assumed to present interpretation difficulties (Catt, 1991) and for a long time received minor attention. Recent studies of thick loessic deposits of the last glaciation enhanced significantly the paleoclimatic signal from the interstadial paleosols due to continuous dense sampling schemes for multiproxy analyses and instrumental dating (Antoine et al., 2001, 2013; Terhorst et al., 2015). The most detailed paleosol series of MIS3–MIS2 were correlated with the interstadials of the GISP curves (Haesaerts et al., 2010).

Geographical distribution of the known Pleistocene paleopedological records is strongly heterogeneous. The Eurasian Loess Belt provides a continuous west–east chain of sections from Western Europe to Chinese Loess Plateau allowing long distance correlations (Haesaerts and Mestdagh, 2000; Rutter et al., 2003; Frechen et al., 2009; Karimi et al., 2011). Extensive loess cover of the Eastern European Plain hosts numerous sections which provide detailed record of alternating eolian sedimentation and pedogenesis (in many cases – cryogenic) as a response to the climate change throughout the Late Pleistocene (Bogutsky, 1986; Velichko, 1990; Morozova and Nechaev, 1997). The area to the north of the Loess Belt, directly affected by strong glacial and periglacial processes of the last glaciations, until now has produced very scarce evidence of the Late Pleistocene paleopedogenesis. Recently, some MIS3 soil relicts were identified very close to the limits of the late Valday glaciation in center-north European Russia (Rusakov and Korkka, 2004; Rusakov and Sedov, 2012). They demonstrated pedogenetic features quite different from those of the synchronous loessic paleosols more to the south.

In the Trans-Ural regions, the data about Pleistocene paleosols are more fragmentary. In particular, central and northern Western Siberia, the middle and lower Ob' basin, is still “terra incognita” for the Quaternary paleopedology: to our knowledge, no publications about Pleistocene soil development in this region are available. This lack of paleopedological results is partly due to still incomplete documentation of the Quaternary sediments and geological formations of this remote and severe region, where geological research mostly deals with oil and gas problems. Moreover, it might be also related to the traditional scheme of the Quaternary geological history of Western Siberia, put forward half a century ago by Saks (1953) and further developed over decades by his numerous followers (Zemtsov, 1976; Arhipov, 1997; Grosswald and Hughes, 2002). This scheme indicated a vast continental ice sheet in the northern West Siberian lowlands during the Last Glaciation, as a continuation of the North European ice sheet. Glacial erosion and sedimentation were supposed to provide little chance for preservation of paleosols, so nobody searched for them. More recently, the traditional viewpoint was strongly challenged by several research groups, which offered results indicated very limited extent of glaciers in Siberia in the Late Pleistocene even during the Last Glacial Maximum – Sartan Cryochron (Svendsen et al., 2004; Velichko et al., 2011; Sheinkman and Plyusnin, 2014).

Sharing these alternative ideas, we further speculated that they imply the possibility for the development and preservation of non-glacial sedimentary and paleopedological records in this area. This was our first motivation to look for the Pleistocene paleosols in the Middle Ob' Basin. Our research hypothesis was defined as follows: supposing the absence of Sartanian (MIS2) glacial erosion and sedimentation in the north of Western Siberia, preservation of the earlier Karga (MIS3) paleosols is possible on the higher Pleistocene alluvial terraces of the Ob' river system. The objective of our research was to identify these paleosols within alluvial sedimentary sequences and extract pedological and biological proxies of MIS3 paleoenvironments. In this paper, we present the results of the initial study from one key section, focused on the following particular tasks:

- to understand the interrelation of paleosols with the hosting geoforms and embedding deposits in order to establish their chrono- and morphostratigraphic position;
- to identify pedogenetic processes, which took part in the development of the paleosol, to utilize them further for paleolandscape reconstruction. We expect to detect responses to global climate changes as well as effects of local geomorphological and tectonic processes;
- to extract paleobotanical (pollen, macroremains, phytoliths) and paleoentomological proxies of past environmental conditions and further compare them with the paleopedological record; and
- to compare studied units with the correlative loessic paleosols of the neighboring regions of Southern Siberia, already provided with extensive datasets (Frechen et al., 2005; Zykina and Zykin, 2003, 2008) to infer geographic variability of the Pleistocene soil cover.

2. Materials and methods

2.1. Study area: geographical localization and landscape characteristics

Our research has been conducted in the basin of the Vakh River, one of the major right-hand tributaries of the Ob' River, which comprises the main structure of the regional hydrographic net in Western Siberia. The Ob' River flows from the Altay Mountains to the Arctic Ocean, generally in the northern direction. However, it has a sub-latitudinal segment in the middle part of the valley, which cuts the West-Siberian Plain from the east to the west at 61–62°N (Fig. 1). To the north of this segment, an extensive gentle upland area is located, the Siberian Uval (“Sibirskie Uvali” in Russian). Its surface has an average altitude of 120–149 m a.s.l., and stretches parallel to the Ob' River, also in latitudinal direction. The Vakh River starts from Verhnetazovskaya Upland near the eastern edge of Siberian Uval, flows south-west and, and reaches the Ob' at the eastern edge of its sub-latitudinal segment.

The present day climate of the Vakh Basin is cool continental. Climate monitoring (2007–2011) carried out at the meteorological station “Glubokiy Sabun” on the territory of the Natural Reserve Park “Siberian Uval” show mean annual temperature of −3.7 °C with quite strong seasonal shift from roughly −41 °C in the coldest month (February) to +17.2 °C in the warmest (June) (Korkin et al., 2014). Mean annual precipitation is about 499 mm, with a maximum of 100 mm in August. The major part of moisture comes from the Atlantic with the western winds (Kazachkova, 1982). Vegetation corresponds to the sub-zone of the Middle Taiga (boreal coniferous forests). The forest stands are dominated by *Pineta sylvestris*, *Pineta sibiricae*, *Piceeta obovatae*, *Lariceta sibiricae*, *Betuleta pubescentis* and *Tremuleta* (Kukurichkin and Neshtaev, 2004), which occupy relatively drained positions. Swamps are widespread (40% of the territory) both on the lower terraces and on the poorly drained flat areas of the uplands: oligotrophic types with *Sphagnum* are dominant. Modern soils under forest are Podzols on the sandy deposits and specific Stagnosols and Gleysols on the loamy materials. Swamps are dominated by Histosols. Concerning the geological background, the study area is a young part of the West-Siberian plate, with Perm-Triassic and older crystalline basement overlain

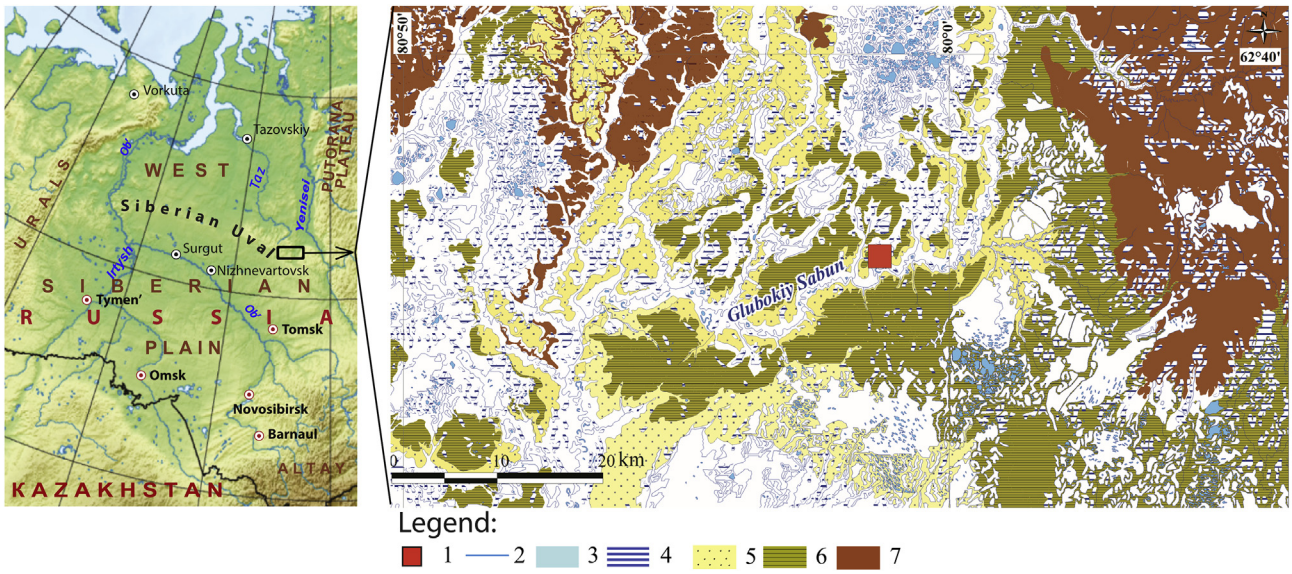

Fig. 1. Geographical localization and geomorphological background of the study site. 1) Location of the exposure "Zeleniy Ostrov", 2) rivers, 3) lakes, 4) oligotrophic swamps, 5) alluvial plain 100–120 m a.s.l. 6) alluvial plain 120–130 m a.s.l. 7) alluvial plain 130–150 m a.s.l.

by a 2.7 km thick mantle of Meso-Cenozoic sediments (Geologicheskaya karta, 1984), predominantly of marine origin. The upper layers of the sedimentary sequence accumulated during the Quaternary, when cyclic climatic changes with extensive cold intervals (cryochrons) gave rise to strong cryogenic processes. The predominantly sandy Quaternary sediments covering the study area have been an object of intensive discussion. The traditional approach developed by the school of Saks (1953) associated these sediments with glacial, fluvio-glacial and limno-glacial settings and processes. These ideas are currently challenged because recent research completely revised the extent of the Late Pleistocene glaciers in Northern Eurasia. An alternative viewpoint was developed since the 1960s, predominantly by the geologists and geocryologists of Moscow Lomonosov University who associated the Quaternary deposits of the northern part of the West Siberian Plain with alluvial, lagoon and epi-continental marine environments (Popov, 1967; Lazukov, 1989). The uplift of the sediment sequences was attributed to tectonism (Kuzin, 2005).

In the middle reaches of the Ob' basin, the most complete Quaternary sedimentary sequences are found in the body of the terrace having a surface at an altitude of 120–140 m a.s.l. The relative height of the terrace is about 40 m. Its surface is discontinuous: the residual terrace blocks are surrounded or dissected by the lower terraces and floodplain. When such blocks are subjected to intensive lateral erosion in the outside of the major river bends they generate high and steep cliffs (locally called "gora") which provide excellent outcrops. At present the terrace bodies are not frozen, because in the study area permafrost has patchy distribution, and its islands have been restricted to swampy peatlands. The continuous permafrost boundary is located some 300 km to the north (Vasil'chuk and Vasil'chuk, 2014). During the summer field seasons of 2013 and 2014, we undertook the field survey of the outcrops formed by the Vakh River and its right-hand tributaries and discovered various exposures of well-preserved paleosols, incorporated in the Late Pleistocene sedimentary sequences.

2.2. Field and laboratory research strategies and techniques

The study site (62°29′26.5″N, 81°51′30.3″E) named "Zeleniy Ostrov" ("the Green Island " in Russian), located on the right-hand bank of the brook Glubokiy Sabun, a right-hand tributary of the Vakh River (Fig. 1) was selected for the detailed field and laboratory research. The field description was focused on the depositional characteristics of the sedimentary strata and pedogenetic properties of the paleosols; color of soil genetic horizons was established according to the Munsell Soil Color Charts (1994). For horizon designation, we followed the Guidelines of FAO (2006) and classification of paleosol and modern soil was done according to WRB (IUSS Working Group WRB, 2014).

Two layers: paleosol humus horizon (layer 6) and sediment with detritus and fossil insects (within layer 2) provided enough organic materials for conventional radiocarbon dating of the total organic carbon. Radiocarbon dating was carried out in the Novosibirsk Radiocarbon Laboratory of the Siberian Branch RAS. The ^{14}C decay period of 5570 y has been used to calculate the ages, from 1950. Conversion of the dates into calendar units has been carried out with the Calib Rev 6.1.0 calibration program.

Different sampling schemes were applied for different laboratory methods. All horizons of the outcrop were sampled for the particle size analysis. Only soil horizons were sampled for soil chemical study (pH, exchangeable cations, organic matter), humus horizons of modern soil and paleosol – for composition of humus, paleosol horizons – for micromorphology. For paleobiological research, we took samples from the most "promising" layers: for palaeobotany – paleosol horizons: layers 6 (385–415 cm) and 7 (415–435 cm)) as well as loamy layers 4 (165–335 cm) and 5 (335–385 cm); for phytoliths – upper paleosol horizon – layer 6 (two samples of layer 6, from the depth 385–395 cm и 405–415 cm); for the entomofauna upper paleosol horizon – layer 6 (385–415 cm). We also included the results on fossil insects, sampled earlier from a thin lens of organic debris in the same exposure but at some distance from the profile reported here (Zinovyev and Nesterkov, 2003). The second radiocarbon date corresponds to the same organic debris. The lens forms part of a sandy bed which correlates with layer 2.

Particle size analysis included sieving for sand and gravel and gravity sedimentation in water with pipette probe for silt and clay with previous dispersion by $Na_4P_2O_7$; the fraction limits were established following Kachinskiy (1965) (Fig. 3). These limits are rather similar to those of WRB (IUSS Working Group WRB, 2014),

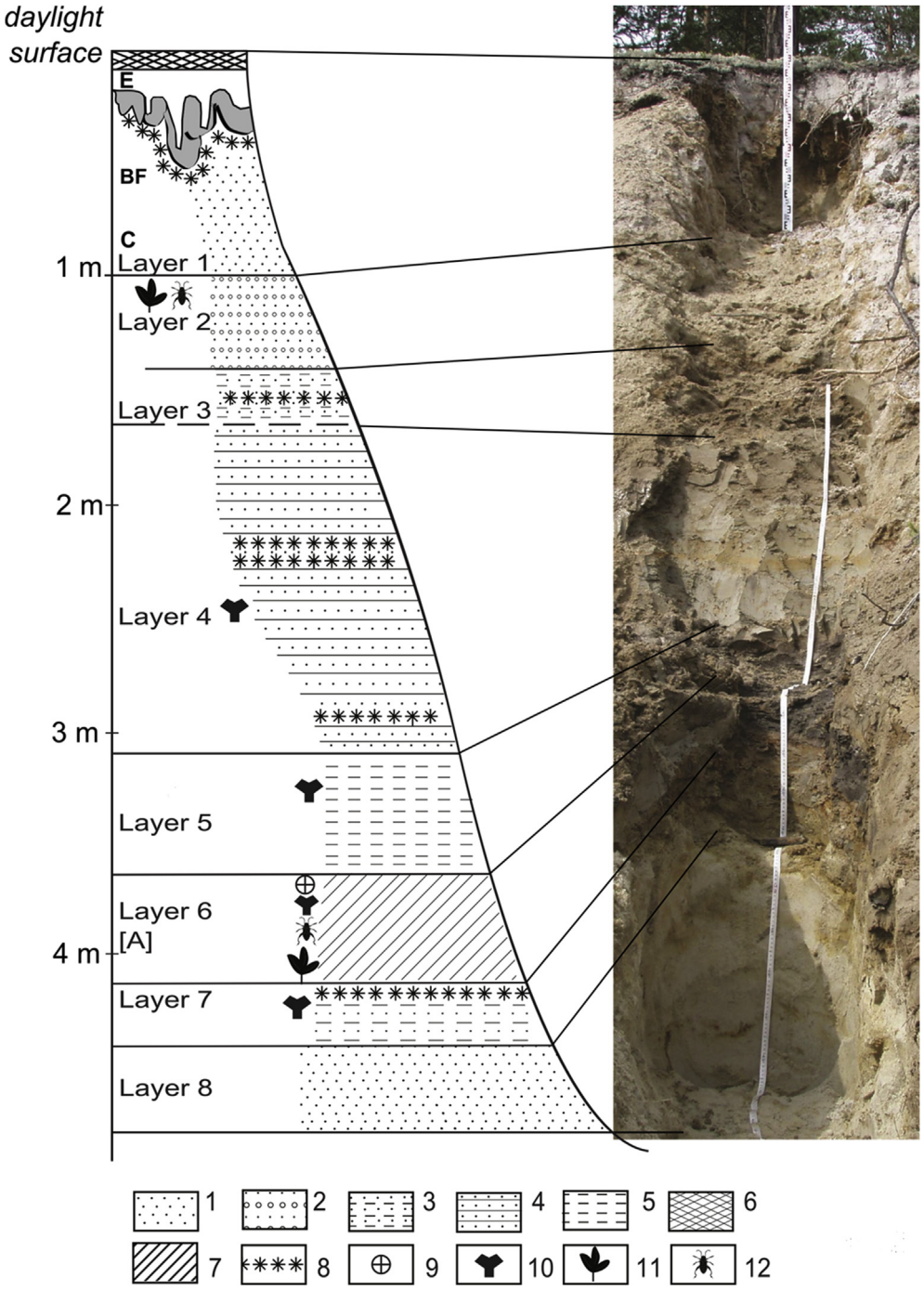

Fig. 2. The scheme of the section Zeleniy Ostrov. 1) Sand, 2) sand with pebbles, 3) silty sand, 4) loam, 5) clay, 6) organomineral Folic horizon of modern Podzol, 7) paleosol humus horizon, 8) Fe nodules, 9) samples for C14, 10) samples for palynological and botanical macroremains analyses, 11) samples for phytoliths, 12) samples for fossil insects.

but the following discrepancies should be marked: 1) the limit of clay fraction of Kachinskiy (1965) – 0.001 mm is smaller than the limit of clay of WRB (IUSS Working Group WRB, 2014) – 0.002 mm; and 2) the upper limit of sand of Kachinskiy (1965) – 1 mm is smaller than that of WRB (IUSS Working Group WRB, 2014) – 2 mm, thus the fraction "very coarse sand" of WRB (IUSS Working Group WRB, 2014) is not included within the sand fractions of Kachinskiy (1965).

pH was measured in water and KCl extracts by inoLab 740 apparatus, exchangeable Ca^{2+} and Mg^{2+} – in the NH_4OAc solution (methods analogous to that recommended by WRB (IUSS Working Group WRB, 2014)). Organic carbon content was estimated by wet oxidation with K bichromate following Tyurin (1966). Fractions of humus were separated by the method of Ponomareva and Plotnikova (Plotnikova and Orlova, 1984). Thin sections from paleosol samples with undisturbed structure were studied under an Olympus petrographic microscope and described following the concepts and terminology of Bullock et al. (1985) and Stoops (2003).

Palaeobotanical analysis included studies of botanical macroremains, pollen, and phytoliths. For macroremains analysis, the sediment was sieved on 500 and 200 μm sieves and analyzed under

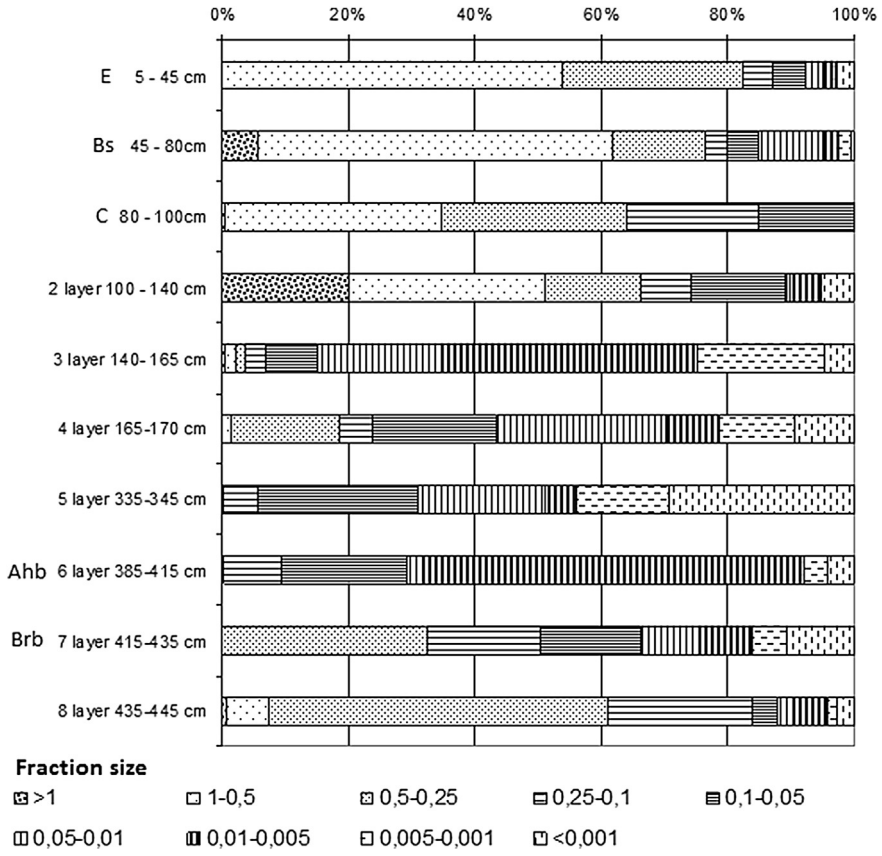

Fig. 3. Particle size distribution of the section Zeleniy Ostrov.

stereomicroscope. For palynological analysis, 2 cm^3 of the sediment from each sample were treated by cold HCl (37%), cold HF (60%) for one night, acetolysis, and sieved on meshes 200 and 10 μm. The remaining pellet was stored in the glycerin and studied under 400× or 1000× magnification. Spores of Lycopodium (Batch number 1031) were added as an exotic marker for determination of pollen concentration. Base sum of pollen counts was minimum 300 total pollen grains, further used for calculation of percentages. However, in layer 4 only 270 pollen in total were found. Pollen taxonomy was based on Beug (2004). Beside pollen, other organic microbiomorphs known as non-pollen palynomorphs were counted (Van Geel, 1978; Shumilovskikh et al., 2015). Their percentages are calculated on base of the pollen sum. The palynological diagram was made using C2 (Juggins, 2007). Phytoliths were first concentrated by flotation in heavy liquid (mixture of Cd and K iodides solutions with density 2.3) and then observed under optical and scanning electronic microscopes (Golyeva, 2001).

Fossil insects were recovered according to the standard procedure (Kiselev, 1987), from the samples containing organic detritus, after wet sieving on the sieve with 0.5 mm opening. Fragments identifiable to genus or species were mounted on special cassettes. The identification was based on comparison of insect remains with the modern analogues from the entomological collection of Institute of Plant and Animal Ecology Ural Branch, Russian Academy of Sciences. Data on the modern geographical distribution and ecological requirements of the encountered *Coleoptera* were obtained from Kryzhanovskij et al. (1995) and Sher and Kuzmina (2007). For interpretation we also used the earlier results on the regional entomofauna (Zinovyev and Nesterkov, 2003).

3. Results

3.1. Section stratigraphy, morphology and dating

The scheme of the studied exposure is presented in Fig. 2, with complete field description provided in Table 1. The section is capped by the well-developed profile of a Podzol consisting of diagnostic horizons typical for this soil type. We observed: AO – horizon including both sandy mineral material and partly decomposed plant debris together with abundant charcoal; E (Albic horizon) – bleached eluvial horizon; and Bs (Spodic horizon) – intensively pigmented in yellow–brown and "coffee" colors by illuvial humus and ferruginous substances. This contrasting horizon sequence was derived from the sandy sediments represented by the pale-yellow C horizon at the bottom of the soil profile.

The Podzol profile overlies a thick sedimentary package (layers 2–5) which show a clear trend towards increasing fine materials with depth. Upper layer 2 consists of laminated coarse sand with some inclusions of stony material – medium- and large pebbles, and medium boulders. However, at the base of the layer the sandy grains become finer. In the next layer 3, an admixture of loam to sand has been registered, whereas layer 4 has loamy texture. Layer 5 is rich in clay. All these layers show clear lamination, sometimes marked with ferruginous nodules or stripes. Thin seams enriched with organic detritus were found within layer 2.

Layers 6 and 7 comprise the profile of the buried paleosol. Layer 6 is dark, colored by organic pigment and contains plant detritus. We interpret it as a buried humus horizon, Ahb. Layer 7, shows mottled pale greenish grey – yellow pigmentation and was identified as a buried gleyic horizon – Brb. A thick uniform sedimentary

Table 1
Field description of the "Zeleniy Ostrov" section.

№ of layer; index of soil horizon		Depth, cm	Field morphological description
1	AO	0–5	Black (10YR 2/1), includes partly decomposed plant debris: pine needles, lichen tissues, etc; mineral sandy material increase downwards, the lower boundary is highlighted by a thin discontinuous black seam of charcoal
	E	5–45	White (7.5YR 8/1), bleached sand with few small black charcoal particles; living tree roots are common (about 2% by volume)
	Bs	45–80	Intensive reddish–yellow (7.5YR 7/8), dark-brown (7.5YR 3/4) near the upper boundary, colour intensity gradually decreases with depth, sandy
	C	80–100	Pale yellow sand with few small black (<2 mm) Mn mottles
2		100–140	Pale brown coarse sand with cross-bedded lamination, includes pebbles (1–5 cm), sand becomes finer towards the bottom
3		140–165	Pale-brown (colour becomes darker towards the bottom) loam, horizontal lamination is marked with ferruginous nodules
4		165–335	Brown (yellow–brown near the bottom) loam, horizontal lamination is marked by ferruginous nodules
5		335–385	Pale-greyish silty clay, with large (up to 4 cm) rusty ferruginous nodules and mottles; in the middle and lower part horizontal stripes pigmented with iron oxides.
6	Ahb	385–415	Dark bluish – gray (10B 4/1), bluish black (10B 2.5/1) when moist, silty clay, compacted but with high plasticity, abundant plant detritus, faint smell of H2S.
7	Brb	415–435	Light greenish gray (5GY 7/1) with yellow-rusty mottles, silty loam, in the upper part – inclusions of material of the overlying horizon.
8		435– …	Pale yellowish-brown, medium sand, the horizontal lamination is marked with sub-horizontal wavy Fe-Mn nodules

layer of laminated medium sand forms the base of the section (Fig. 2, Table 1).

Two conventional radiocarbon dates has been obtained from the total organic carbon of the paleosol humus horizon (layer 6, 385–415 cm) and from the above-mentioned lens of detritus in the sandy unit below (layer 2, see Fig. 2). The measured radiocarbon age in the paleosol Ahb horizon is 22100 + 325 ^{14}C BP (SOAN-7550), which after calibration produced the date 25,693–27,748 cal BP. In the sample from organic detritus within the layer 2 the measured radiocarbon age is 10,780 + 70 ^{14}C BP (LE-8972), which after calibration produced the date 12,756–12,956 cal BP.

3.2. Physical and chemical characteristics of soils and sediments

The studied section shows clear differentiation of particle size distribution: the upper sedimentary package with the modern soil is sandy, the middle part with the paleosol is silty loam, whereas the basal layer is sandy. All horizons of Podzol within layer 1 and layer 2 have more than 60% coarse and medium sand fractions (1–0.25 mm). The underlying sedimentary package (layers 3–5) as well as paleosol (layers 6 – Ahb horizon, and 7 – Brb horizon) are characterized by elevated silt (0.05–0.001 mm) content ranging from 23 (layer 7) to 80% (layer 3). Sand increases in the basal layer, dominated by medium sand particles (0.5–0.25 mm) (Fig. 3).

The modern soil is slightly acid, and pH varies between 5.3 and 5.8, gradually increasing from bottom to top. The paleosol has much higher pH values: 6.6–6.7. Exchangeable cations also show sharp differences: the paleosol contains 10 to 100 times more exchangeable Ca^{2+} and Mg^{2+}, than the modern Podzol (Table 2).

Humus content and composition differs greatly in the modern Podzol and the paleosol. The buried humus Ahb horizon has more than 15% total organic carbon compared to 2% in the surface AO horizon. Humus of the Podzol is dominated by fulvic acids. The ratio of humic to fulvic acids is very low: 0.33 in the Ah horizon. In the paleosol Ahb horizon, this ratio is close to 1, indicating much higher content of humic acids. Elevated values of fraction 2 (linked to Ca^{2+}) of both humic (HA2) and (especially) fulvic (FA2) acids are observed in the paleosol humus horizon (Table 3).

Table 3
Composition of humus in Ah horizons of modern soil and paleosol of "Zeleniy Ostrov" section.

Soil horizons; Layer no.	Depth, cm	Humus fractions, % of C_{org}				C_{HA}/C_{FA}
		HA	HA2	FA	FA2	
Modern soil						
Ah; 1	0–5	5.08	2.13	15.44	2.02	0.33
Buried paleosol						
Ahb; 6	385–415	28.00	12.09	29.71	17.25	0.94

HA – Humic acids, FA – Fulvic acids.

Table 2
Chemical properties of modern soil and paleosol of "Zeleniy Ostrov" section.

Soil horizons; Layer no.	Depth, cm	pH_{H_2O}	pH_{KCl}	Exchangeable cations meq/100 g		Corg %
				Ca^{2+}	Mg^{2+}	
Modern soil						
Ah; 1	0–5	5.81	4.91	1.05	0.50	2.16
E; 1	5–45	5.48	4.73	0.10	0.05	–
Bs; 1	45–80	5.32	4.14	0.10	0.05	–
C; 1	80–100	5.29	3.39	0.10	0.05	–
Buried paleosol						
Ahb; 6	385–415	6.64	5.74	16.6	7.46	15.87
Brb; 7	415–435	6.55	5.54	11.12	3.85	1.8

3.3. Micromorphological observations

Under the microscope the material of the paleosol humus Ahb horizon is very compact, with very few visible pores: very small packing voids between organic particles and very few thin fissures. Within the groundmass, two major components are discriminated: 1) organic material consisting of coarse plant fragments of variable sizes (up to ~ 1 mm), moderately decomposed (fragmentation, partial dark-brown pigmentation), cellular structure is well preserved in the larger fragments – tissue residues; organic fine material is present mostly as cell residues and polymorphic amorphous fine material; dark organic pigment is found in minor quantities as admixture to other materials and has patchy distribution; 2) mineral material dominated by silicate silt with a minor amount of clay and few sand grains (mostly quartz).

Both major components show uneven distribution: some areas are enriched with organic detritus, and others with mineral material. In the "organic" microareas plant fragments demonstrate diversity of sizes and orientation, among organic particles admixture of mineral grains is present (Fig. 4a). Within the "mineral" microareas, grain size sorting is frequently observed: coarse sandy grains are concentrated in the clusters whereas neighboring areas consist only of silt and clay with admixtures of plant detritus. Circular orientation of clay is sometimes observed in the fine mineral areas; the remainder has stipple-speckled orientation (Fig. 4b). Pedofeatures are presented by the iron oxides concentration shaped in a curved stripe – probably part of a concentric ferruginous nodule (Fig. 4c). In this thin section, we found a cluster of neoformed pyrite crystals, opaque isometric grains with characteristic golden luster. Transparent crystals with grey interference color surrounding the pyrite cluster are identified as gypsum, a typical product of pyrite oxidation (Fig. 4d).

The lower part of the Ahb horizon has less organic detritus and a larger proportion of mineral material which also is characterized by segregation of sand grains in clusters (Fig. 4e). Here, we observed deformation and fragmentation of the elongated plant fragments (Fig. 4f).

The underlying Brb horizon consists predominantly of very compact mineral matrix dissected with very few thin fissures. Unlike the overlying humus horizon, the sand grains do not form clusters, and they are uniformly distributed in the silty-clay matrix giving rise to single to double spaced porphyric c/f related distribution (coarse grains immersed in fine-grained matrix) (Fig. 4g). In this horizon, we found carbonate pedofeatures, circular or radial intergrowth of well shaped calcite crystals (Fig. 4h).

3.4. Botanical macroremains

Sieving of samples for botanical macroremains analysis demonstrates that layers 4, 5 and 7 are composed mainly of sands and contain very low amounts of plant material in the form of unidentifiable plant detritus (Table 4). In layers 4 and 5, *Sphagnum* leaves occur sporadically. Layer 6, the paleosol Ahb horizon, differs from other layers considerably by its organic composition with a main component of *Eriophorum* vegetative remains, indicating formation of *Eriophorum* peat. Local vegetation was composed by *Eriophorum*, *Carex*, *Luzula*, *Potentilla supina*-type and trees such as *Betula nana* and *Salix* (Fig. 5).

Table 4
Results of botanical macroremains analysis of "Zeleniy Ostrov" section.

Layer (depth, cm)	Volume, ml	Botanical macroremains
4 (165–335 cm)	230	Sporadically plant detritus and *Sphagnum* leaves
5 (335–385 cm)	170	Sporadically plant detritus and *Sphagnum* leaves
6 (385–415 cm)	260	Seeds: *Eriophorum* (3), *Luzula* sp. (7), *Potentilla supina*-type (3), *Carex nigra*-type (22), *Betula* (5) Vegetative remains: *Eriophorum* remains (numerous), *Betula/Salix* leave fragments, *Salix* bud scales
7 (415–435 cm)	170	Plant detritus

3.5. Phytoliths

Very few phytoliths were recovered from the humus horizon, probably due to separation problems caused by abundance of the organic materials. The majority of the recovered phytoliths (4 particles) belong to conifer trees (Fig. 5i). One elongated particle (probably from grasses) was found. Other opaline microfossils are a very few sponge spicules and fragmented diatom shells.

3.6. Palynology

Palynological analysis demonstrates differences in pollen content of different layers (Fig. 6). As expected, sedimentary layers 4, 5 and paleosol Brb horizon – layer 7 have very low pollen concentrations, varying between 800 and 2200 pollen/cm^3, whereas in the paleosol Ahb horizon – layer 6 concentrations reach up to 26,000 pollen/cm^3.

Pollen spectra differ between layers. The lowest layer 7 is characterized by high percentages of non-arboreal pollen (NAP) exceeding 50% and dominated by *Artemisia* and Poaceae and a variety of herbs and ferns. Arboreal pollen (AP) is mainly represented by *Betula* sect. *Albae*, *Betula* sect. *Nanae/Fruticosae* and *Pinus* subgen. *Diploxylon*. Green algae Zygnemataceae and *Bortyococcus* are present.

In the paleosol Ah horizon (layer 6), percentages of *Artemisia* and Poaceae decrease, with increases in Cyperaceae, Chenopodiaceae and Caryophyllaceae and other herbs. AP include *Pinus* subgen. *Haploxylon*, *Picea* and *Larix*, with increasing conifers in pollen spectra in comparison to layer 7, along with increased percentages of *Sphagnum*.

The next layer 5 changes considerably from the lower layers by increased AP up to 69%, which is composed by 25% *Pinus* subgen. *Diploxylon*, 8% *Pinus* subgen. *Haploxylon*, 10% *Betula* sect. *Nanae/Fruticosae* and 21% *Betula* sect. *Albae* together with conifers *Larix* and *Picea*, pioneer tree *Populus*, wet habitats indicators *Alnus/Duschekia* and *Salix*, and heathland indicator *Vaccinium*-type. In NAP, *Artemisia*, Cyperaceae and Chenopodiaceae drop to 5, 2 and 1% respectively with increased Poaceae (19%) and occurrence of several herbs such as *Mentha*-type, Brassicaceae, *Rhinanthus* group, *Matricaria*-type and *Thalictrum*. This layer has the highest amount of *Sphagnum* spores accompanied by *Bryophytomyces sphagni* and tardigrade eggs.

In layer 4, percentages of *Pinus* subgen. *Diploxylon* drop to 3%, *Betula* sect. *Nanae/Fruticosae* reach 23% and *Betula* sect. *Albae* – 30%. NAP spectra are similar to layer 5, but fewer herbs are present. Green algae *Botryococcus* and *Pediastrum* are detected.

3.7. Fossil insects

Analysis of two sub-fossil insect faunas (Table 5, Fig. 7) demonstrates differences between complexes from the paleosol Ahb horizon (layer 6) and from younger detritus-rich sediment within the layer 2. Insect assemblage found in layer 6 is characterized by small number of fragments (23) and individuals (12). Despite the scarcity of insect remains in this sample, the

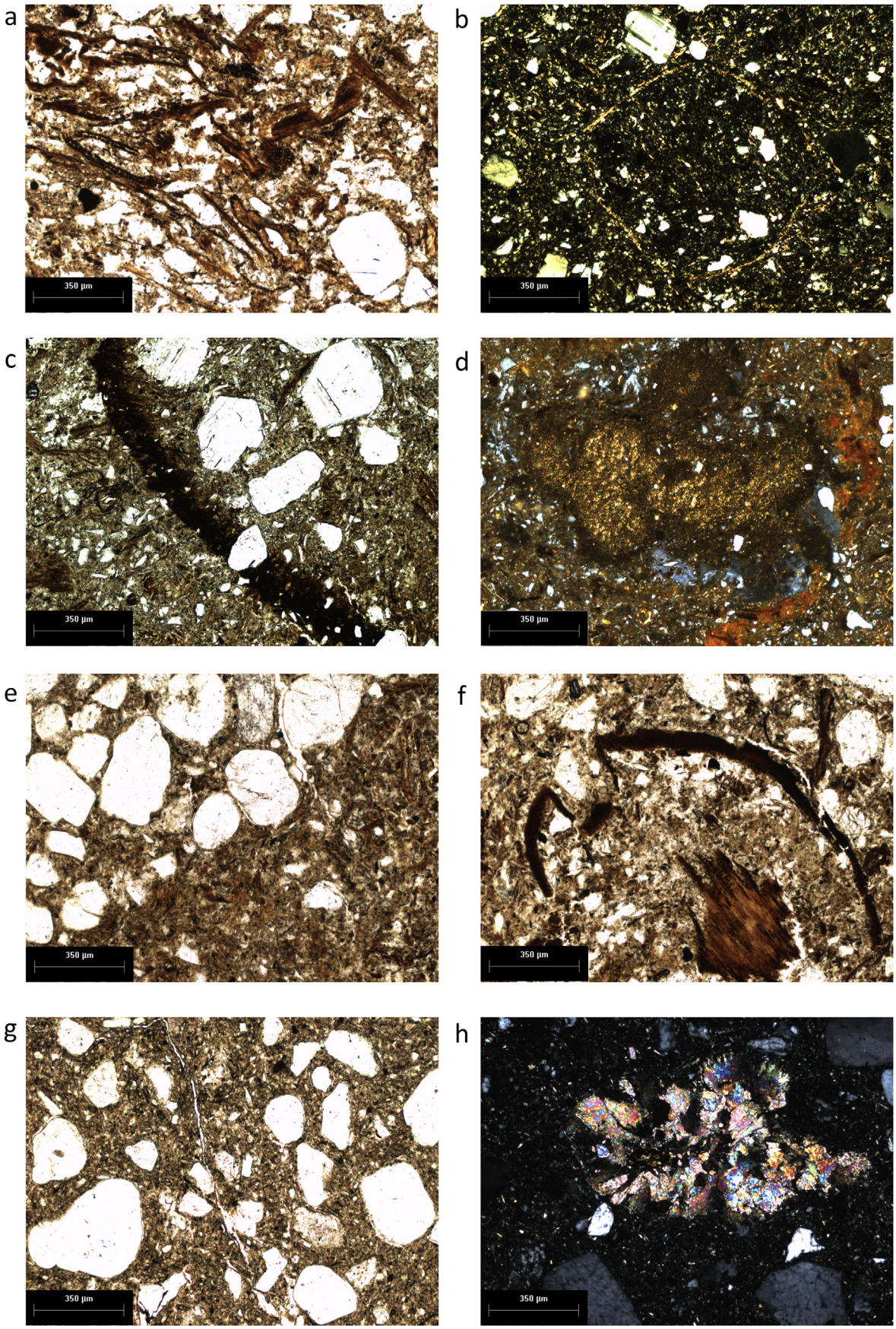

Fig. 4. Micromorphology of the paleosol (see explanation for each photo in the text).

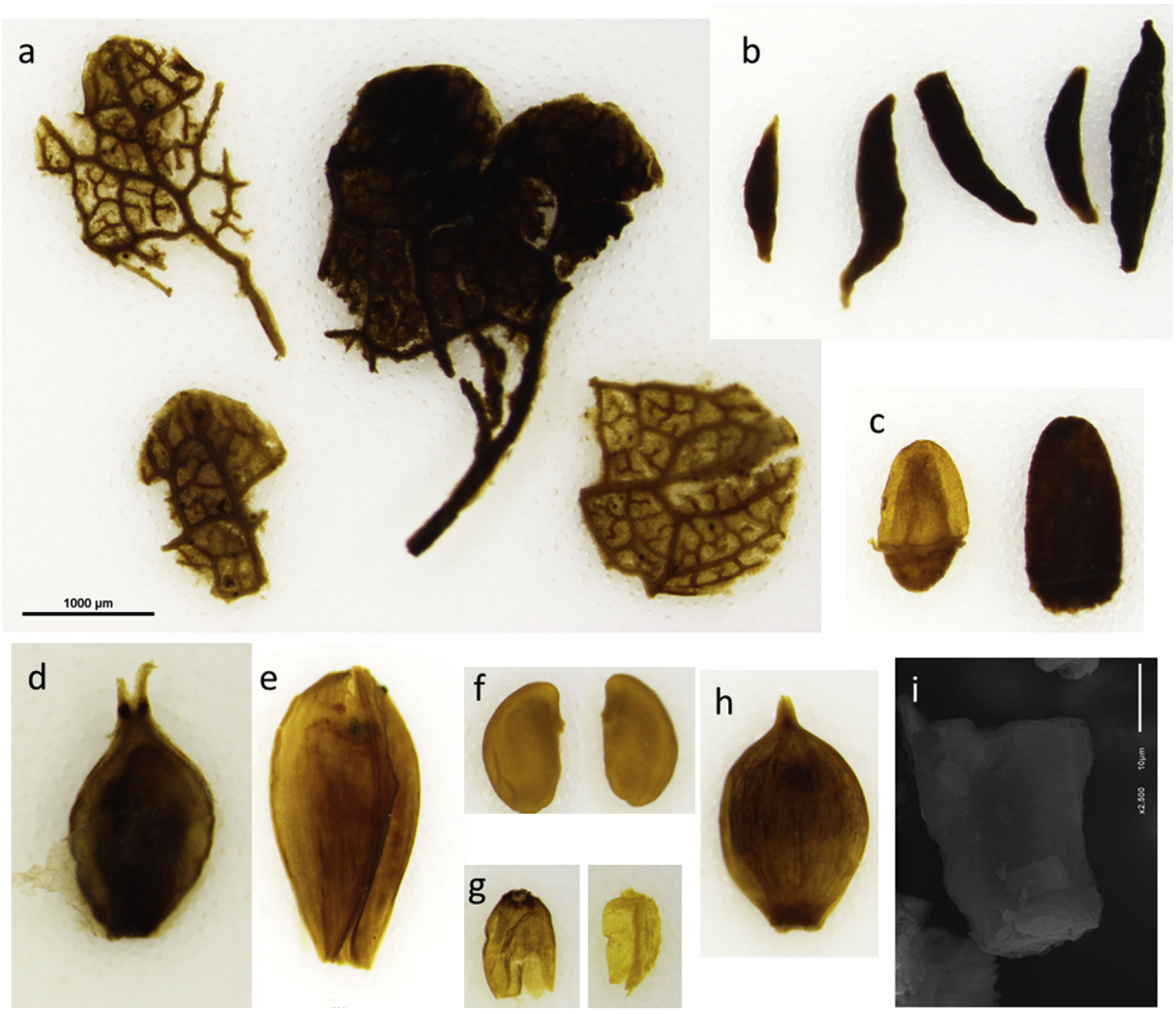

Fig. 5. Botanical macroremains and phytolith from layer 6: a) *Betula nana*, leaves; b) *Eriophorum* sp., vegetative remains; c) *Salix* sp., bud scales; d) *Betula* sp., nutlet; e) *Eriophorum* sp., nutlet; f) *Potentilla* sp., nutlet; g) *Luzula* sp., nutlet; h) *Carex* sp., nutlet. Scale: 1000 µm = 1 mm. i) conifer phytolith, SEM.

species composition is typical for modern tundra (*Tachinus arcticus*, *T. brevipennis*, *Amara alpina*, *Pterostichus* (*Cryobius*) cf. *pinquedineus*).

Insect fauna from layer 2 consists of a large number of fragments (383) and individuals (185). It consists of boreal (*Notiophilus fasciatus*, *Pterostichus adstrictus*, *Calathus micropterus*, *Chlaenius costulatus* etc.), intrazonal (*Clivina fossor*, *Lorocera pilicornis*, *Elaphrus riparius*, *Bembidion quadrimaculatum*, *Acidota crenata*, *Chrysolina lapponica*, etc.) species with the presence of some subarctic beetles (*Diacheila polita*). Most abundant ecological groups are "aquatic" (8.1%) and "near-aquatic" (47.6%); "taiga" and "mesic tundra" species account for 6.5% and 4.3% of the total respectively. Species composition of this layer reflects the presence of riparian forests adjoining sandy banks of a river and riparian shrub associations represented by willows (leaf beetles *Chrysomela lapponica* (Fig 7.3), *Conioctena* sp. (Fig 7.5), weevil *Lepyrus volgensis*) and birch (weevil *Trichapion simile*). Some ground beetles indicate forest communities (*Pterostichus adstrictus*, *Calathus micropterus*, *Cymindis vaporariorum*, *Notiohilus fasciatus*). The ground beetle *Chlaenius costulatus* (Fig 7.4) inhabits swamp forests and peat soils. The subarctic ground beetle *Diacheila polita* (Fig 7.1) prefers moss litter.

4. Discussion

4.1. Section chronology and stratigraphy: sedimentary environment of paleosol formation and burial

Although at present only 2 radiocarbon dates are available for the studied section, they provide an idea about paleosol chronology. The radiocarbon date of organic material from the paleosol humus horizon 25,693–27,748 cal BP corresponds to the transition between MIS3 (the Karga thermochron stage in Western Siberia) and MIS2 (the Sartan cryochron). According to the existing models of radiocarbon signal generation in the soil organic matter, the ^{14}C date of paleosol humus indicaes the final stage of the paleosol development, close to its burial (Matthews, 1985). Consequently the major part of the paleosol formation period took place before the date. This means that it could be attributed to late MIS3, the Karga thermochron.

Such chronological attribution of the paleosol suggests that the overlying sequence of laminated loamy and sandy sediments was formed during the last cryochron – Sartan (MIS2). The radiocarbon date from the organic detritus found in a seam within the upper sand bed gives an age of 12,756–12,956 cal BP, which corresponds

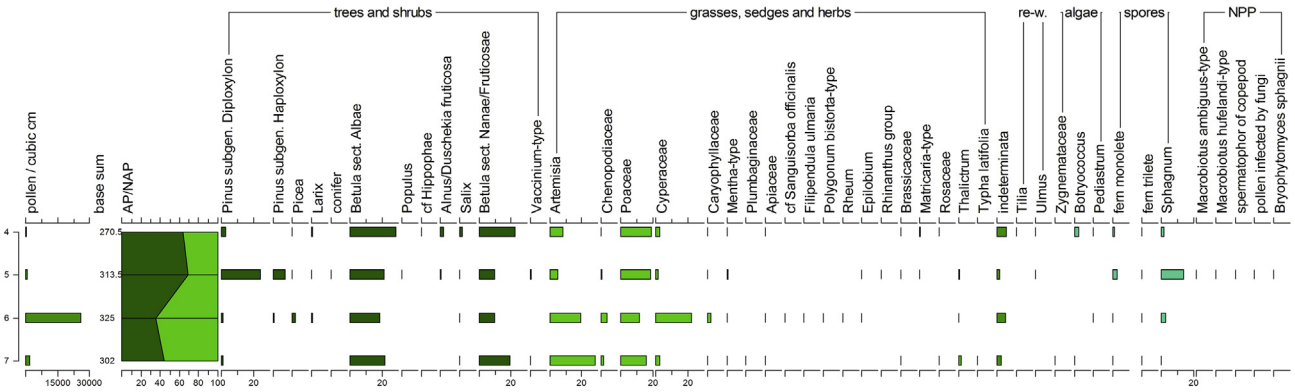

Fig. 6. Palynological diagram of Zeleniy Ostrov site.

to the end of the Sartan and agrees with the proposed chronology. The sedimentological characteristics of the deposits overlying the paleosol: well developed lamination with parallel and crossed bedding, high degree of sorting, and predominantly rounded grains in the sand layers point to a fluvial or lacustrine sedimentary environment. The presence of pebbles and even rounded boulders in the upper sandy unit is a puzzling feature. Some researchers argue that stony material of this kind provides a strong argument in favour of past glacier advance. However, these stones are not associated with glacial sediments or geomorphological bodies. They are widely spread within the Middle Ob basin, being included in the bodies of the river terraces, the surface of which has been situated at the altitude of about 120 m a.s.l., i.e. as if the stones have been "immersed" in laminated and well-sorted alluvial strata. We suppose them to be typical drop-stones transported by ice-floe drift through the Paleo-Ob' and Paleo-Yenisei river system in the periods of the highest floods and during some marine ingressions along their valleys. During these events of high water stand streams with ice-floes, and stony material included in them, could spill over not so high watersheds and spread in the Ob'-Yenisei interfluve. Further studies on minerology of pebbles might shed light on their nature.

Very high silt content is characteristic for the loamy sediments which host the paleosol and provide its parent material. Eolian dust deposition participated in the development of this sedimentary package.

The thick basal sand layer underlying the paleosol is supposed to be formed during the Zyryan Time (MIS4–late MIS5), as in sections in other parts of the Vakh River a few radiocarbon dates have already given ages more than 40 ka cal BP. The uninterrupted character of sedimentation in the whole thickness of this layer allows us to conclude, judging by average rate of deposition, that its base was formed not earlier than in the beginning of MIS5 (Sheinkman and Plyusnin, 2014).

4.2. Pedogenesis and paleoecological significance of the buried soil: regional paleopedological correlations

The most prominent pedogenetic processes which defined profile morphology of the studied paleosol are:

1) Accumulation of partly decomposed plant material. This process is evident in the Ahb – paleosol humus horizon. Macroscopic observations detect high quantities of organic detritus in this horizon. Under microscope in thin section this material is present as coarse organic particles with preserved tissue morphology. However, a large part of these particles has signs of decomposition – fragmentation and substitution by organic polymorphic fine material. Some organic matter was further transformed into colloidal humus – organic pigment, mixed with mineral components, which provides the dark color of the horizon. The overall organic carbon content in the paleosol is much higher than in the modern soil, despite the inevitable loss of part of the organic matter due to diagenetic decomposition.
2) Gleyzation – a group of phenomena related to Fe and Mn mobilization in reduced soil environment. This process is most evident in the Brb horizon, due to the typical pale greenish-gray color pattern with yellow mottles. In thin sections we found redoximorphic features: ferruginous mottles and nodules, in the Ahb horizon. The type and distribution of redoximorphic color pattern in the paleosol profile corresponds to gleyic (long-term water saturation) rather than to stagnic (short-term saturation by surface water) properties. This combination of properties is typical for soil development under water saturated environments which hampers decomposition of organic material and initiates gleyzation. Originally, in the field this soil was classified as a Gleysol (organic matter content in the Ahb horizon does not reach the level required for Histosols) (WBR, 2014).

Further comparison of the buried paleosol with the recent surface soil highlights major a difference between modern and past pedogenetic processes and factors, the main interest of this research. The recent soil on top of the studied section is an Albic Podzol, formed by the processes of leaching, acidification and eluvial–illuvial redistribution of Fe and Al, bound to soluble organic substances. This set of processes requires good internal drainage and free percolation of soil solutions. Saturation with water and redoximorphic processes are uncommon for these soils: we did not find these features in the studied Podzol. Recent soil formation is in good agreement with the geomorphological and geological conditions of pedogensis: on an elevated terrace surface on sandy sediments which provide excellent drainage conditions.

Thus, the contrasting qualitative difference between properties of the paleosol and modern soil indicates a major change of drainage conditions. Buried gleyic paleosols were observed below modern Podzols in Zeleniy Ostrov as well in a number of other sections on the drained terrace surfaces. Different texture of soil parent material could be responsible for this difference. Paleosols are developed in silty loams, whereas modern soils form in sandy sediments. However, modern loamy soils formed in Western Siberia under Middle Taiga forests in Western Siberia are different. Tonkonogov (2010) reports soils with bleached upper horizons and strong eluvial/illuvial differentiation of iron (Svetlozems) to be formed on loams in the upland positions under taiga in Western Siberia. According to the reported characteristics and genetic

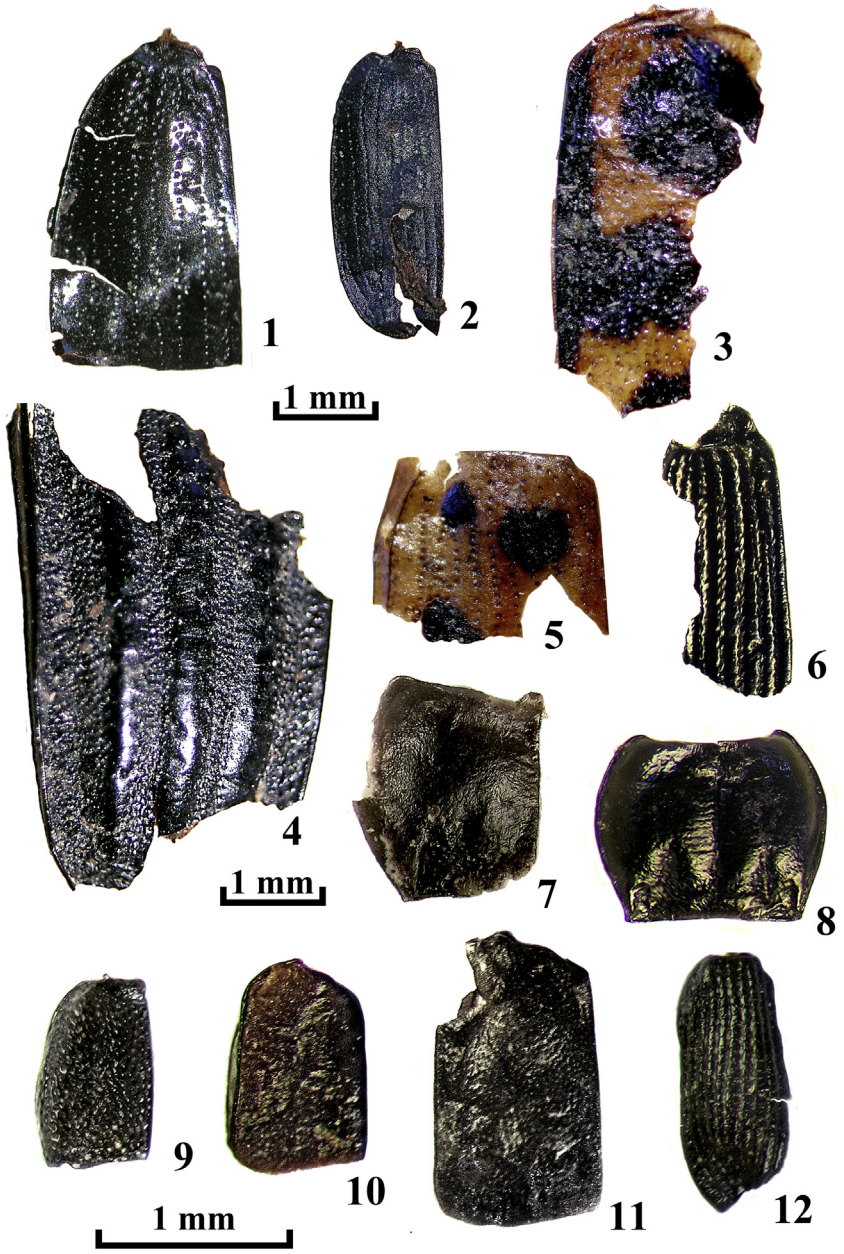

Fig. 7. Insect remains found in Zeleniy ostrov site. 1. *Diacheila polita* Faldermann, 1835, left elytron (layer 2); 2. *Bembidion* (*Odontium*) cf. *striatum* (Fabricius, 1792), left elytron (layer 2); 3. *Chrysomela lapponica* Linnaeus, 1758, right elytron (layer 2); 4. *Chlaenius costulatus* Motschulsky, 1859, left elytron (layer 2); 5. *Gonioctena* sp., left elytron (layer 2); 6. *Pterostichus* (*Cryobius*) cf. *pinguedineus* Eschscholtz, 1823, left elytron (layer 6); 7. *Amara* (*Curtonotus*) *alpina* (Paykull, 1790), left half of pronotum (layer 6); 8. *Pterostichus* (*Cryobius*) cf. *pinguedineus* Eschscholtz, 1823, pronotum (layer 6); 9. *Stenus* sp. left elytron (layer 6); 10. *Tachinus brevipennis* J. Sahlberg, 1880, left elytron (layer 6); 11. *Tachinus arcticus* (Motschulsky, 1860), left elytron (layer 6); 12. *Isohnus arcticus* Korotyaev 1977, left elytron (layer 6).

interpretation these soils could be affiliated with Stagnosols, characterized by temporal saturation with surface water. They differ from the paleosols, which demonstrate strong redoximorphic features caused by prolonged groundwater saturation (Gleyic properties of WRB (IUSS Working Group WRB, 2014)).

As paleopedological interpretation is based on an actualistic approach, the knowledge of recent soils is of major importance for the search of the modern analogues on the regional scale and within broader geographical limits (Bronger and Catt, 1998). Strong gleying is observed in the loamy soils of tundra zone in the northern West Siberian Plain (Vasilevskaya et al., 1986; Khrenov, 2011) where continuous water saturation is conditioned by permafrost. On the continental scale, gleyzation above shallow a permafrost table is typical for soils of tundra, forest-tundra and colder continental taiga ecosystems of Northern Eurasia (Gerasimova et al., 1996). In the global perspective Gleyic properties are considered to be common in Cryosols, developing upon saturation with water during the thaw period (FAO, 2001). The redoximorphic processes are active in the Cryosols of the Arctic soil zone, showing maximum in the Low Arctic and Subarctic Tundra and decreasing in the coldest sector of the High Arctic (Polar Desert) (Goryachkin et al., 2004; Bockheim, 2015).

We speculate that presence of permafrost could be responsible for hampering internal soil drainage and switching on the redoximorphic processes during formation of the MIS3 paleosol on the high Pleistocene terraces of the Vakh basin. This interpretation

Table 5
List of Coleoptera from the Zeleniy Ostrov site. The numbers opposite each taxon indicate the minimum number of individuals in the sample.

Taxon	Sample 1 layer 5	Sample 2 layer 6a	Ecological group[a]
Order Coleoptera			
Dytiscidae			
Agabus sp.	1		aq
Coelambus sp.	1		aq
Hydroporus sp.	1		aq
Dytiscidae indet.	2		aq
Carabidae			
Carabus aeruginosus Fischer von Waldheim, 1822	1		ta
Carabus odoratus Motschulsky, 1844	2		mt
Carabus (*Morphocarabus*) sp.	1		other
Pelophila borealis (Paykull, 1790)	2		na
Notiophilus fasciatus Maklin, 1855	1		ta
Diacheila polita Faldermann, 1835	6		mt
Elaphrus riparius (Linnaeus, 1758)	1		na
Lorocera pilicornis (Fabricius, 1775)	2		na
Clivina fossor (Linnaeus, 1758)	5		na
Dyschiriodes sp.	1		na
Dyschirius globosus Herbst, 1784	1		na
Dyschirius obscurus (Gyllenhal, 1827)	1		na
Bembidion cf. *striatum* (Fabricius, 1792)	1		na
Bembidion quadrimaculatum (Linnaeus, 1761)	1		na
Bembidion fellmanni (Mannerheim, 1823)	1		na
Bembidion (*Ocydromus*) sp.	1		na
Bembidion sp.	1		na
Patrobus assimilis Chaudoir, 1844	2		na
Patrobus septentrionis Dejean, 1828	4		na
Pterostichus adstrictus Eschscholtz, 1823	1		ta
Pterostichus cf. *dilutipes* Motschulsky, 1844	1		ta
Pterostichus (*Cryobius*) cf. *pinguedineus* Eschscholtz, 1823		6	mt
Pterostichus sp.	1		other
Calathus micropterus Duftschmid, 1823	2		ta
Agonum fuliginosum (Panzer, 1809)	4		na
Agonum versutum Sturm, 1824	1		na
Amara quenseli (Schoenherr, 1806)	1		me
Amara (*Curtonotus*) *alpina* (Paykull, 1790)		1	dt
Amara (*Curtonotus*) *torrida* Panzer, 1706.	1		me
Amara sp.	1		other
Chlaenius costulatus Motschulsky, 1859	1		ta
Cymindis vaporariorum (Linnaeus, 1758)	1		ta
Cymindis macularis Fischer von Waldheim, 1824	1		ta
Carabidae indet.	3		other
Hydrophilidae			
Hydrobius fuscipes (Linnaeus, 1758)	9		aq
Liodidae			
Liodes sp.	1		other
Staphylinidae			
Acidota crenata (Fabricius, 1793)	1		na
Acidota cf. *quadrata* (Zetterstedt, 1838)	1		na
Acidota sp.	6		na
Olophrum rotundicolle (C.R.Sahlberg, 1827)	3		na
Olophrum sp.	8		na
Omaliinae indet.	15		na
Quedinus sp.	2		other
?*Quedinus* sp.	4		other
?*Mycetoporus* sp.	1		other
Tachinus cf. *arcticus* (Motschulsky, 1860)		1	mt
Tachinus cf. *brevipennis* J.Sahlberg, 1880		2	mt
Tachyporinae indet.	3		other
Lathrobium sp.	2		na
Ocypus sp.	1		other
Stenus sp.	8	1	na
Aleocharinae indet.	1		other
Staphylinidae indet.	3		other
Scarabaeidae			
Aegialia abdita Nikritin, 1978	2		na
Scarabaeidae indet.	1		other
Byrrhidae			
Byrrhus pilula Linnaeus, 1758.	3		ta
?*Curimopsis* sp.	1		other
Morychus sp.	1		me
Simplocaria sp.	2		na
Scirtidae			
?*Cyphon* sp.	4		na
Heteroceridae			
Heteroceris sp.	1		na
Elateridae			
Hypnoidus rivularius (Gyllenhal, 1808)	2		na
Elateridae indet.	1		other
Chrysomelidae			
Gonioctena sp.	2		sh
Chrysomela lapponica Linnaeus, 1758	2		sh
Chrysolina staphylea (Linnaeus, 1758)	2		sh
Chaetocmema sp.	1		sh
Chrysomelidae indet.	1		other
Curculionidae			
Notaris aethiops (Fabricius, 1793)	3		na
Tournotaris bimaculata (Fabricius, 1792)	1		na
Phyllobius sp.	1		sh
Lepyrus volgensis Faust, 1890	1		sh
Phytobius sp.	2		me
Hypera sp.	1		me
Isochnus cf. *arcticus* Korotyaev, 1977		1	dt
Rhynchaenus sp.	2		sh
Curculionidae indet.	3		other
Apionidae			
Trichapion simile (Kirby, 1811)	2		sh
Coleoptera indet.	3		other
Order Trichoptera			
Trichoptera indet.	1		aq
Order Diptera			
Diptera indet	10		other
Insecta indet.	1		other
Total number of individuals	185	12	

[a] Ecological groups of insects: aq – aquatic species; na – riparian and near aquatic species, this group include also strongly hygrophilous species, do not rigidly connected to any bodies of water but living in wetland habitats; ta – taiga species; dt – dry tundra inhabitants; mt – mesic tundra inhabitants; sh – shrub group, species associated with willows and birch; me – insects living in meadows, mostly in the forest zone.

changes the position of this paleosol within the WRB classification: it should be named a Reductaquic Cryosol (IUSS Working Group WRB, 2014). Similar interpretation (permafrost effect) and classification (as Cryosol) of the Late Pleistocene gleyic paleosols was presented earlier: 1) for "Tundragley" corresponding to MIS3/MIS2 transition in the Austrian loess-paleosol sequences (Terhorst et al., 2015) and 2) for MIS3 "Gleysols" in the north Central Russia (Rusakov and Sedov, 2012).

Presence of permafrost supposes a colder climate than present during the paleosol development. In agreement with this supposition, micromorphological features give evidence of frost-induced features in the upper paleosol horizon: separation of coarse and fine material, disorientation and deformation of plant fragments and mixing with the mineral material (Van Vliet-Lanoë, 1998, 2010).

The neutral soil reaction of paleosols, in contrast to acidity in modern soils, as well as dominance higher proportions of humic acids and humus components linked to Ca^{2+} point to restricted leaching, more continental and less humid climate during the paleosol formation period. These inferences agree with the presence of secondary carbonates, gypsum and iron sulphides which are reported as typical authigenic minerals of extreme continental permafrost landscapes (Siegert, 2005). Continental tundra or tundra-steppe ecosystems as well as some cold continental boreal forests could host such pedogenesis. However, pyrite formation in

soils could be caused by influence of the brackish saline waters rich in sulfates (FAO, 2001; Mees and Stoops, 2010). Marine transgressions along the valleys of Paleo-Ob' and Paleo-Yenisei river systems were possible during and after paleosol formation. In this case gypsum could be interpreted as a product of pyrite oxidation in the presence of carbonates.

Comparison with synchronous paleosols from the Siberian loess sequences located to the southeast of the study area show differences between paleosol profiles. Paleosols of Iskitim pedocomplex which correspond to MIS3 are underdeveloped Chernozems corresponding to cool steppe environments (Zykina and Zykin, 2003). A clear similarity is observed between the studied paleosol and MIS3 paleosols in the Upper Volga Basin, at proximal latitudinal position on the opposite western side of the Urals. The latter paleosols also expose strong gleyic features and accumulation of plant remains, mixed with mineral materials (Rusakov and Korkka, 2004; Rusakov and Sedov, 2012) This geographical diversity of synchronous paleosols provide interesting hints to reconstruction of MIS3 soil zonality on the East European and West Siberian Plains.

4.3. Biological indicators of paleoenvironments: integration with the paleopedological and sedimentary records

Palynological analysis demonstrates a clear difference of layers 6 and 7 from layers 4 and 5, suggesting different environmental and/or climatic situations during the sediment deposition. Similarity in pollen spectra of layers 6 and 7 suggests that they were deposited under similar rather dry conditions. The dominance of *Artemisia* and Poaceae together with *Betula* sect. *Nanae/Fruticosae* indicates presence of open tundra-steppe with birch and possibly willow on dry, well drained areas. If pine and *Betula* sect. *Albae* pollen can be explained by local stands and/or long-distance transport, pollen of *Picea* and *Larix* indicate presence of spruce and larch stands relatively close to the site. Especially, larch pollen is well-known for poor transport, indicating local presence of trees. At water-logged sites, wetlands with Cyperaceae and *Sphagnum* could be developed as in layer 6. In contrast to rather dry conditions, suggested from pollen spectra, presence of open water, possibly temporarily, at both layers is indicated by *Typha latifolia* pollen and algae Zygnemataceae, *Pediastrum*, and *Botryococcus*. Macroremains analysis clearly shows that layer 6 represents wetlands formed by *Eriophorum* (Fig. 4b and e), *Carex* (Fig. 4h), *Potentilla* (Fig. 4f) and *Luzula* (Fig. 4g) with birch (Fig. 4a and d) and willow (Fig. 4c). Well-preserved plant remains strongly suggest that decomposition was rather low due to the water-logged position of the site for a longer period. The phytholith analysis suggests presence of conifers on the site (Fig. 4i), which is not confirmed by macroremains but by the presence of *Larix* pollen. In general, layers 6 and 7 suggest decreasing wetness, and layer 7 was formed under drier conditions, indicated by maxima of steppe indicators *Artemisia* and Poaceae. In contrast, in layer 6 Cyperaceae reach maxima due to local development of sedge wetland. The paleobotanical record agrees well with the paleopedological proxy: in general, both point to a cold continental tundra-steppe ecosystem. In particular, the presence of wetland and water indicators corresponds to features of gleyization, which are especially strong in layer 6. We attribute paleosol hydromorphism to water logging by permafrost and thus interpret it as a signal of cold climate. However, steppe pollen taxa such as *Artemisia* and Poaceae indicating dry climatic conditions in layer 7 are in agreement with paleopedological characteristics such as neutral soil reaction, abundance of humic acids and Ca-bound components within soil organic matter, and the presence of secondary carbonates. These inferences are also consistent with the sedimentological characteristics of the deposits associated with the paleosol. Abundance of silty material in the paleosol Brh horizon and in overlying sediments suggest eolian dust input. This sedimentary process is typical for drier environments with open discontinuous vegetation. The data on fossil insects agree completely with the proposed interpretation for layer 6: the species recovered from the paleosol humus horizon are typical for tundra ecosystems.

The tendency of increasing wetness continues in layers 5 and 4, characterized by sharp decrease of *Artemisia* and dominance of Poaceae and *Betula* sect. *Nanae/Fruticosae*, suggesting development of bushy tundra in the area and, therefore, regional wet conditions. Such wet conditions could be explained by worse drainage caused by permafrost and/or lower evaporation. Increased amounts of pollen of conifers and *Betula* sect. *Albae* indicate presence of forest stands in the area or increased amount of long-distance transport due to decrease of forest cover in the region. Locally, *Sphagnum* is clearly indicated by *Sphagnum* leaves (Table 2) and spores (Fig. 5) together with spores of the *Sphagnum* fungal parasite *Bryophytomyces sphagnii* and tardigrade eggs of *Macrobiotus ambiguus*-type and *Macrobiotus hufelandi*-type, which can be often found in moss environments (Shumilovskikh et al., 2015). Presence of (temporary) open water in layer 5 is indicated by spermatophors of copepods. Surprisingly, the sediment is composed mainly of sand, which possibly can indicate that *Sphagnum* peat lenses were very fine. Layer 4 does not contain sphagnophilous indicators, but *Sphagnum* spores and leaves, which could be re-deposited by water. Furthermore, possible re-deposition of material or long distance transport is indicated by the presence of pollen of deciduous broadleaved *Ulmus* and *Tilia* in layers 4 and 5. Open water at the site during layer 4 deposition is indicated by green algae *Botryococcus* and *Pediastrum*.

The following layer 2 allows environmental reconstructions based on beetle assemblages (Fig. 6). Occurrence of *D. polita* indicates cooler than present climate: the southern boundary of the modern range of this subarctic beetle in West Siberia does not reach this territory. This species is represented by a considerable number of fragments (17, total number of individuals 6 – see Table 3), which eliminates accidental finding and suggests that this species existed in favourable conditions. Therefore, the joint occurrence of *D. polita* with taiga species in the sample indicates forests of northern taiga type, presently distributed 200–300 km to the north of the studied territory, and cooler than present climate. The entomological material recovered from the upper part of the section (layer 2), regarding its abundance and specific taxa, indicates the presence of riparian forests of northern taiga type, cooler than present climatic conditions, but milder than those of the paleosol formation period. According to the date, we attribute this layer to the warm intervals of the end of MIS2 (Greenland interstadial 1, Bølling-Allerød).

Continuous fluvial sedimentation of predominantly sand material also indicates a humid environment and thus agrees with the palynological and entomological proxies. The general trend of the vegetation development at Zeleniy Ostrov shows dominance of open and rather dry tundra-steppe with some forests at the end of MIS3, changing to wet bushy forest-tundra during the transition to MIS2, and spread of northern taiga at the end of MIS2 during the Bølling-Allerød.

In general, the results from Zeleniy Ostrov are in agreement with regional data. Hubberten et al. (2004) suggest relatively mild climate conditions in the West Siberian Plain during the final stage of the Middle Weichselian. Lipovka section (58°N, 67°E) on the Tobol river provides evidence of in situ larch trees from peat layers dated to 30–31 ka BP (Hubberten et al., 2004) and a forest-tundra environment. In West Siberia, the period between 20 and 24 ka BP is characterized as cool but relatively humid (Hubberten et al., 2004).

Further northeast in the Laptev Sea region, last glacial landscapes were more open in comparison to Zeleniy Ostrov and were represented by dense grass-sedge-*Artemisia* tundra-steppe during Middle Weichselian and sparse grass-sedge tundra-steppe during the Late Weichselian (Andreev et al., 2011). For example, pollen diagrams from Bykovsky Peninsula and Cape Mamontovy Klyk reveal the dominance of Poaceae with some Cyperaceae, *Artemisia*, Brassicaceae and Caryophyllaceae, indicating open tundra- and steppe-like environments existing due to the cold and dry summer. Similar to Zeleniy Ostrov, accumulation of sediment here occurred under aquatic conditions. Insect records from Mamontovy Khayata cliff on the Bykovsky Peninsula (Sher et al., 2005) reveals a trend to a more humid environment at 34–24 ka with an increasing role of wet tundra habitats and decrease of dry tundra. The period 24–15 ka is characterized by dominance of arctic tundra insects, indicating cooler summers. Several other sediment records from the Laptev Sea region have hiatuses between 30 and 17 ka.

In the Baikal region (Bezrukova et al., 2010), the Kotokel record attests that the period between 30 and 16 ka was the coldest and driest during the last 50 ka. The interval at ~30–24 ka BP is characterized by dominance of *Artemisia* and Poaceae, indicating fully established steppe with herbaceous tundra communities. From ~23 ka, development of herbaceous tundra-steppe with increased taiga biome component is indicated.

In the most continental region at present, Verkhojansk, the general vegetation dynamics recorded in lake Billyakh (Müller et al. 2010) characterize the period between 31 and 13 ka as the coldest and driest with dominance of tundra-steppe with shrubby vegetation and larch, indicating that climate conditions were not harsh enough to prevent tree growth. During ~26–13 ka, *Artemisia* has lower percentages in comparison to the period before, whereas Cyperaceae and Poaceae increase and tundra biomes dominate, possibly indicating wetter conditions during this period.

In general, vegetation and climate reconstruction from the section Zeleniy Ostrov is in agreement with regional data, showing rather cool and dry continental conditions during the transition MIS3–MIS2. Thereby, rather dry tundra-steppe conditions dominated at the end phase of MIS3, changing to more wet tundra conditions to MIS2 and the spread of taiga at the end of MIS2.

Acknowledgements

We appreciate financial support from Tyumen State Gas and Oil University and RFBR grant 15-34-50645_2015. L. Shumilovskikh was supported by D.I. Mendeleev Scientific Fund Program of Tomsk State University and RFBR (16-35-60083). We thank Felix Bittmann and Tanja Reiser from Lower Saxony Institute for Historical Coastal Research for their help with identification of botanical macroremains and Jaime Díaz from the Institute of Geology, UNAM for preparing soil thin sections.

References

Andersen, K.K., Azuma, N., Barnola, J.-M., Bigler, M., Biscaye, P., Caillon, N., Chappellaz, J., Clausen, H.B., Dahl-Jensen, D., Fischer, H., Flückiger, J., Fritzsche, D., Fujii, Y., Goto-Azuma, K., Grønvold, K., Gundestrup, N.S., Hansson, M., Huber, C., Hvidberg, C.S., Johnsen, S.J., Jonsell, U., Jouzel, J., Kipfstuhl, S., Landais, A., Leuenberger, M., Lorrain, R., Masson-Delmotte, V., Miller, H., Motoyama, H., Narita, H., Popp, T., Rasmussen, S.O., Raynaud, D., Röthlisberger, R., Ruth, U., Samyn, D., Schwander, J., Shoji, H., Andersen, M.-L.S., Steffensen, J.P., Stocker, T., Sveinbjörnsdóttir, A.E., Svensson, A., Takata, M., Tison, J.-L., Thorsteinsson, T., Watanabe, O., Wilhelms, F., White, J.W.C., 2004. High-resolution record of Northern Hemisphere climate extending into the last interglacial period. Nature 431, 147–151.

Andreev, A.A., Schirrmeister, L., Tarasov, P.E., Ganopolski, A., Brovkin, V., Siegert, C., Wetterich, S., Hubberten, H.-W., 2011. Vegetation and climate history in the Laptev Sea region (Arctic Siberia) during Late Quaternary inferred from pollen records. Quaternary Science Reviews 30, 2182–2199.

Antoine, P., Rousseau, D.-D., Zöller, L., Lang, A., Munaut, A.-V., Hatté, C., Fontugne, M., 2001. High-resolution record of the last Interglacial–glacial cycle in the Nusslochloess–palaeosol sequences, Upper Rhine Area, Germany. Quaternary International 76–77, 211–229.

Antoine, P., Rousseau, D.-D., Degeai, J.-P., Moine, O., Lagroix, F., Kreutzer, S., Fuchs, M., Hatté, C., Gauthier, C., Svoboda, J., Lisa, L., 2013. High-resolution record of the environmental response to climatic variations during the last interglacial–glacial cycle in Central Europe: the loess–palaeosol sequence of Dolní Věstonice (Czech Republic). Quaternary Science Reviews 67, 17–38.

Arhipov, S.A., 1997. Record of Late Pleistocene geological events in west Siberia. Russian Geology and Geophysics 38 (12), 1891–1911.

Beug, H.-J., 2004. Leitfaden der Pollenbestimmung. Verlag Dr. Friedrich Pfeil, München.

Bezrukova, E.V., Tarasov, P.E., Solovieva, N., Krivonogov, S.K., Riedel, F., 2010. Last glacial-interglacial vegetation and environmental dynamics in southern Siberia: chronology, forcing and feedbacks. Palaeogeography, Palaeoclimatology, Palaeoecology 296, 185–198.

Bockheim, J.G., 2015. Cryopedology. Progress in Soil Sciences. Springer, Cham Heidelberg New York Dordrecht London.

Bogutsky, A.B., 1986. Antropogenovyje pokrovnyje otlozhenija Volyno-Podolii (Quaternary cover sediments of Volhynia-Podilja). In: Makarenko, D.E. (Ed.), Antropogenovye Otlozhenija Ukrainy. Naukova Dumka, Kiev, pp. 121–132 (in Russian).

Bronger, A., Catt, J.A., 1998. The position of paleopedology in geosciences and agricultural sciences. Quaternary International 51 (52), 87–93.

Bronger, A., Winter, R., Sedov, S., 1998. Weathering and clay mineral formation in two Holocenc soils and in buried paleosols in Tadjikistan: towards a Quaternary paleo-climatic record in Central Asia. Catena 34, 19–34.

Bullock, P., Fedoroff, N., Jongerius, A., Stoops, G., Tursina, T., Babel, U., 1985. Handbook for Soil Thin Section Description. Waine Research Publications, Wolverhampton, U.K.

Catt, J.A., 1991. Soils as indicators of Quaternary climatic change in mid-latitude regions. Geoderma 51, 167–187.

Dodonov, A.E., Sadchikova, T.A., Sedov, S.N., Simakova, A.N., Zhou, L.P., 2006. Multidisciplinary approach for paleoenvironmental reconstruction in loess-paleosol studies of the Darai kalon section, Southern Tajikistan. Quaternary International 152 (153), 48–58.

FAO, 2001. Lecture Notes on the Major Soils of the World. In: World Soil Resources Reports, vol .94. Food and Agriculture Organization of the United Nations, Rome.

FAO, 2006. Guidelines for Soil Description, fourth ed. Food and Agriculture Organization of the United Nations, Rome.

Frechen, M., Kehl, M., Rolf, C., Sarvati, R., Skowronek, A., 2009. Loess chronology of the Caspian lowland in northern Iran. Quaternary International 198, 220–233.

Frechen, M., Zander, A., Zykina, V., Boenigk, W., 2005. The loess record at the section at Kurtak in Middle Siberia. Palaeogeography, Palaeoclimatology, Palaeoecology 228 (3/4), 228–244.

Geologicheskaya karta, 1984. Zapadnosibirskoy Ravnini s prilegayuschimi territoriyami [Geological Map of the West Siberian Plain and Adjacent Areas] M 1: 1500000. Ministry of Geology of the USSR, Moscow.

Gerasimova, M.I., Gubin, S.V., Shoba, S.A., 1996. Soils of Russia and Adjacent Countries: Geography and Micromorphology. Moscow State University, Wageningen Agricultural University, Moscow, Wageningen.

Golyeva, A.A., 2001. Biomorphic analysis as a part of soil morphological investigations. Catena 43, 217–230.

Goryachkin, S.V., Blume, H.P., Beyer, L., Campbell, I., Claridge, G., Bockheim, J.G., Karavaeva, N.A., Targulian, V., Tarnocai, C., 2004. Similarities and differences in Arctic and Antarctic soil zones. In: Kimble, J. (Ed.), Cryosols. Permafrost-affected Soils. Springer, pp. 49–70.

Grosswald, M.G., Hughes, T.J., 2002. The Russian component of an Arctic ice sheet during the last glacial maximum. Quaternary Science Reviews 21, 121–146.

Haesaerts, P., Mestdagh, H., 2000. Pedosedimentary evolution of the last interglacial and early glacial sequence in the European loess belt from Belgium to central Russia. Geologie en Mijnbouw/Netherlands Journal of Geosciences 79 (2/3), 313–324.

Haesaerts, P., Borziac, I., Chekha, V.P., Chirica, V., Drozdov, N.I., Koulakovska, L., Orlova, L.A., van der Plicht, J., Damblon, F., 2010. Charcoal and wood remains for radiocarbon dating Upper Pleistocene loess sequences in Eastern Europe and Central Siberia. Palaeogeography, Palaeoclimatology, Palaeoecology 291, 106–127.

Hubberten, H.W., Andreev, A., Astakhov, V.I., Demidov, I., Dowdeswell, J.A., Henriksen, M., Hjort, C., Houmark-Nielsen, M., Jakobsson, M., Kuzmina, S., Larsen, E., PekkaLunkka, J., Lysså, A., Mangerud, J., Möller, P., Saarnisto, M., Schirrmeister, L., Sher, A.V., Siegert, C., Siegert, M.J., Svendsen, J.I., 2004. The periglacial climate and environment in northern Eurasia during the Last Glaciation. Quaternary Science Reviews 23, 1333–1357.

IUSS Working Group WRB, 2014. World Reference Base for Soil Resources 2014. International soil classification system for naming soils and creating legends for soil maps. World Soil Resources Reports No. 106. FAO, Rome.

Juggins, S., 2007. Software for Ecological and Palaeoecological Data Analysis and Visualisation. User Guide Version 1.5. University of Newcastle, Newcastle upon Tyne.

Kachinskiy, N.A., 1965. Fizika pochvy (The Physics of Soils). Vysshaya shkola Publishers, Moscow (In Russian).

Karimi, A., Frechen, M., Khademi, H., Kehl, M., Jalalian, A., 2011. Chronostratigraphy of loess deposits in northeast Iran. Quaternary International 234, 124–132.
Kazachkova, K.K., 1982. Klimaticheskaya harakteristika zoni osvoeniya nefti i gaza Tyumenskogo severa (The Climatic Characteristic of a Zone of Development of Oil and Gas of the Tyumen North). Gidrometeoizdat, Leningrad.
Khrenov, V.Ya, 2011. Pochvi kriolitozoni Zapadnoy Sibiri (Soils of Western Siberia Cryolithozone). Nauka, Novosibirsk.
Kiselev, S.V., 1987. Field sampling for entomological analysis: the Manual (Moscow Univ). Complex Biostratigraphic Investigations 21–26.
Korkin, S.E., Korkina, E.A., Storchak, T.V., Hodzhayeva, G.K., 2014. Geoecologichesky monitoring na territorii prirodnogo parka "Sibirskie Uvali" (Geoecological monitoring on the territory of the natural park "Siberian Uval"). Izdatel'stvo Nizhnevartovsk Universitet, Nizhnevartovsk (in Russian).
Kryzhanovskij, O.L., Belousov, I.A., Kabak, I.I., Kataev, B.M., Makarov, K.V., Shilenkov, V.G., 1995. A Checklist of the Ground Beetles of Russia and Adjacent Lands (Insecta, Coleoptera, Carabidae). Pensoft Publishers, Sofia, Moscow.
Kukla, G., An, Z., 1989. Loess stratigraphy in central China. Paleogeography, Palaeoclimatology, Palaeoecology 72, 203–225.
Kukurichkin, G.M., Neshtaev, V.Yu, 2004. Ocherk vodorazdelnih lesov prirodnogo parka "Sibirskie Uvali" (Sketch of the watershed forests of natural park "Sibirskie Uvaly"). In: Ekologicheskie issledovaniya vostochnoi chasti Sibirskih Uvalov [Ecological Researches of the Eastern Part of "Sibirskie Uvaly"]. Priobie Publishers, Nizhnevartovsk, pp. 14–43 (in Russian).
Kuzin, I.L., 2005. Geomofologia Zapadno-Sibirskoy ravnini (Geomorphology of the West Siberian Plain). Gosudarstvennayz polyarnaya academia, S.Petersburg (in Russian).
Lazukov, G.I., 1989. Pleystotsen territirii SSSR (Pleistocene of the Territory of the USSR). Visshaya shkola, Moscow (in Russian).
Matthews, J., 1985. Radiocarbon dating of surface and buried soils: principles, problems and prospects. In: Richards, K., Arlett, R., Ellis, S. (Eds.), Geomorphology and Soils. Allen and Unwin, London, pp. 271–288.
Mees, F., Stoops, G., 2010. Sulphuric and sulphidic materials. In: Stoops, G., Marcelino, V., Mees, F. (Eds.), Interpretation of Micromorphological Features of Soils and Regoliths. Elsevier, Amsterdam, pp. 543–568.
Morozova, T.D., Nechaev, V.P., 1997. The Valdai periglacial zone as an area of cryogenic soil formation. Quaternary International 41 (2), 53–58.
Müller, S., Tarasov, P.E., Andreev, A.A., Tütken, T., Gartz, S., Diekmann, B., 2010. Late Quaternary vegetation and environments in the Verkhoyansk Mountains region (NE Asia) reconstructed from a 50-kyr fossil pollen record from Lake Billyakh. Quaternary Science Reviews 29, 2071–2086.
Munsell soil color charts, 1994. Munsell Color., New Windsor.
Plotnikova, T.A., Orlova, N.Ye, 1984. Use of modification of the Ponomareva-Plotnikova method for determining the nature, composition, and properties of soil humus. Soviet Soil Science 16 (6), 98–108.
Popov, A.I., 1967. Merzlotnie yavlenia v zemnoy kore (Permafrost Phenomena in the Lithosphere). Izdatelstvo MSU, Moscow. P., p. 304
Rusakov, A.V., Korkka, M.A., 2004. The Bryansk fossil soil of the extraglacial zone of the Valday glaciation as an indicator of landscape and soil forming processes in the center of the Russian plain. Revista Mexicana de Ciencias Geologias 21, 94–100.
Rusakov, A., Sedov, S., 2012. Late Quaternary pedogenesis in periglacial zone of northeastern Europe near ice margins since MIS 3: timing, processes, and linkages to landscape evolution. Quaternary International 265, 126–141.
Rutter, N.W., Rokosh, D., Evans, M.E., Little, E.C., Chlachula, J., Velichko, A., 2003. Correlation and interpretation of paleosols and loess across European Russia and Asia over the last interglacial–glacial cycle. Quaternary Research 60 (1), 101–109.
Saks, V.N., 1953. Chetvertichniy period v Sovetskoy Arktike (Quaternary Period of Soviet Arctic). Gidrometeoizdat, Moscow, Leningrad (in Russian).
Sheinkman, V.S., Plyusnin, V.M., 2014. Glaciation of Western Siberia in the siberian system of natural ice. Geography and Natural Resources 3, 22–31.
Sher, A.V., Kuzmina, S.A., 2007. Late Pleistocene beetle records from northern Asia. In: Beetle Records: Lite Pleistocene of Northern Asia. Elsevier, pp. 94–115.
Sher, A.V., Kuzmina, S.A., Kuznetsova, T.V., Sulerzhitsky, L.D., 2005. New insights into the Weichselian environment and climate of the East Siberian Arctic, derived from fossil insects, plants, and mammals. Quaternary Science Reviews 24, 533–569.
Shumilovskikh, L.S., Schlütz, F., Achterberg, I., Bauerochse, A., Leuschner, H.H., 2015. Non-pollen palynomorphs from mid-Holocene peat of the raised bog Borsteler Moor (Lower Saxony, Germany). Studia Quaternaria 32, 5–1.
Siegert, C., 2005. Mineral formation in Sediments Formed in Permafrost Landscapes. Terra Nostra Heft 2005/2: 2nd European Conference on Permafrost. Programme and Abstracts Potsdam, Germany, p. 113.
Stoops, G., 2003. Guidelines for Analysis and Description of Soil and Regolith Thin Sections. Soil Science Society of America, Madison, WI.
Svendsen, J.I., Alexandersson, H., Astakhov, V., Demidov, J., Dowdeswell, J.A., Henriksen, M., Hjort, C., Houmark-Nielsen, M., Hubberten, H., Ingólfsson, Ó., Jakobsson, M., Kjaer, K., Larsen, E., Lokrantz, H., Luunka, E.P., Lysa, A., Mangerud, J., Maslenikova, O., Matioushkov, A., Murray, A., Möller, P., Niessen, F., Saarnisto, M., Siegert, M., Stein, R., Spielhagen, R., 2004. Ice sheet history of northern Eurasia. Quaternary Science Reviews 22, 1229–1271.
Svensson, A., Andersen, K.K., Bigler, M., Clausen, H.B., Dahl-Jensen, D., Davies, S.M., Johnsen, S.J., Muscheler, R., Rasmussen, S.O., Röthlisberger, R., 2006. The Greenland Ice Core Chronology 2005, 15–42 ka. Part 2: comparison to other records. Quaternary Science Reviews 25, 3258–3267.
Terhorst, B., Sedov, S., Sprafke, T., Peticzka, R., Meyer-Heintze, S., Kühn, P., Solleiro Rebolledo, E., 2015. Austrian MIS 3/2 loess-palaeosol records – key sites along a west-east transect. Palaeogeography, Palaeoclimatology, Palaeoecology 418, 43–56.
Tonkonogov, V.D., 2010. Avtomorfnoe pochvoobrazovanie v tundrovoy i taezhnoy zonah Vostochnoevropeyskoy I Zapadno-Sibirskoy ravnini (Automorphic Soil Formation in the Tundra and Taiga Zones of the East European and West Siberian Plains). Dokuchaev Soil Science Institute, Moscow.
Tyurin, I.V., 1966. Voprosi genezisa I plodorodiya pochv (Questions of Genesis and Fertility of Soils). Science, Moscow (in Russian).
Van Geel, B., 1978. A palaeoecological study of Holocene peat bog sections in Germany and the Netherlands, based on the analysis of pollen, spores and macro- and microscopic remains of fungi, algae, cormophytes and animals. Review of Palaeobotany and Palynology 25, 1–120.
Van Vliet-Lanoë, B., 1998. Frost and soils: implications for paleosols, paleoclimates and stratigraphy. Catena 34, 157–183.
Van Vliet-Lanoë, B., 2010. Frost action. In: Stoops, G., Marcelino, V., Mees, F. (Eds.), Interpretation Ofmicromorphological Features of Soils and Regoliths. Elsevier, Amsterdam, pp. 81–106.
Vasil'chuk, Y., Vasil'chuk, A., 2014. Spatial distribution of mean winter air temperatures in Siberian permafrost at 20–18 ka BP using oxygen isotope data. Boreas 43, 678–687.
Vasilevskaya, V.D., Ivanov, V.V., Bogatirev, L.G., 1986. Pochvi severnoy chasti Zapadnoy Sibiri (Soils of the Northern Part of West Siberia). Moscow State University, Moscow.
Velichko, A.A., 1990. Loess-paleosol formation on the Russian Plain. Quaternary International 7 (8), 103–114.
Velichko, A.A., Timireva, S.N., Kremenetski, K.V., MacDonald, G.M., Smith, L.C., 2011. West Siberian Plain as a late glacial desert. Quaternary International 237 (1–2), 45–53.
Zemtsov, A.A., 1976. Geomorfologia Zapadno-Sibirskoy ravnini (severnaya I tsentralnaya chast (Geomorphology of West-siberia Plain (Northern and Central Parts)). Izdatel'stvo Tomskogo Universiteta, Tomsk (in Russian).
Zinovyev, E.V., Nesterkov, A.V., 2003. Novye dannye k izucheniyu chetvertichnyh nasekomyh territorii Zapovedno-Prirodnogo parka "Sibirskie Uvaly" (New data to studying the Quaternary insects from the Natural Reserve park "Sibirskie Uvaly"). In: Ekologicheskie issledovaniya vostochnoi chasti Sibirskih Uvalov [Ecological Researches of the Eastern Part of "Sibirskie Uvaly"]. Priobie Publishers, Nizhnevartovsk, pp. 66–82.
Zykina, V.S., Zykin, V.S., 2003. Pleistocene warming stages in Southern West Siberia: soils, environment, and climate evolution. Quaternary International 106 (107), 233–243.
Zykina, V.S., Zykin, V.S., 2008. The loess-soil sequence of the Brunhes chron from West Siberia and its correlation to global and climate records. Quaternary International 179, 171–175.